Chapter 1

Nuclear pairing: basic phenomena revisited

G.F. Bertsch

Institute for Nuclear Theory and Dept. of Physics, University of Washingtion, Seattle, Washington

I review the phenomena associated with pairing in nuclear physics, most prominently the ubiquitous presence of odd-even mass differences and the properties of the excitation spectra, very different for even-even and odd-A nuclei. There are also significant dynamical effects of pairing, visible in the inertias associated with nuclear rotation and large-amplitude shape deformation.

1. Basic phenomena

In this section I will present some of the basic manifestations of pairing in nuclei, using contemporary sources[1,2] for the experimental data. In later sections, I will describe in broad terms the present-day theoretical understanding of nuclear pairing, emphasizing the many-body aspects rather than the aspects related to the underlying Hamiltonian.

1.1. *Pairing gaps: odd-even binding energy differences*

The basic hallmarks of pair condensates are the odd-even staggering in binding energies, the gap in the excitation spectrum of even systems, and the compressed quasiparticle spectrum in odd systems. To examine odd-even staggering, it is convenient to define the even and odd neutron pairing gaps with the convention

$$\Delta^{(3)}_{o,Z}(N) = \frac{1}{2}(E_b(Z,N+1) - 2E_b(Z,N) + E_b(Z,N-1)), \text{ for } N \text{ odd, (1)}$$

$$\Delta^{(3)}_{e,Z}(N) = -\frac{1}{2}(E_b(Z,N+1) - 2E_b(Z,N) + E_b(Z,N-1)), \text{ for } N \text{ even. (2)}$$

where N and Z are the neutron and proton numbers and E_b is the binding energy of the nucleus. The proton pairing gaps are defined in a similar way. With the above definition, the gaps are positive for normal pairing. The neutron pairing gaps are shown as a function of neutron number in Fig. 1. The data for this plot was obtained from nuclear binding energies given in the 2003 mass table.[1] The upper panel shows the gaps centered on odd N. Typically, the odd-N nuclei are less bound than the average of their even-N neighbors by about 1 MeV. However, one sees that there can be about a

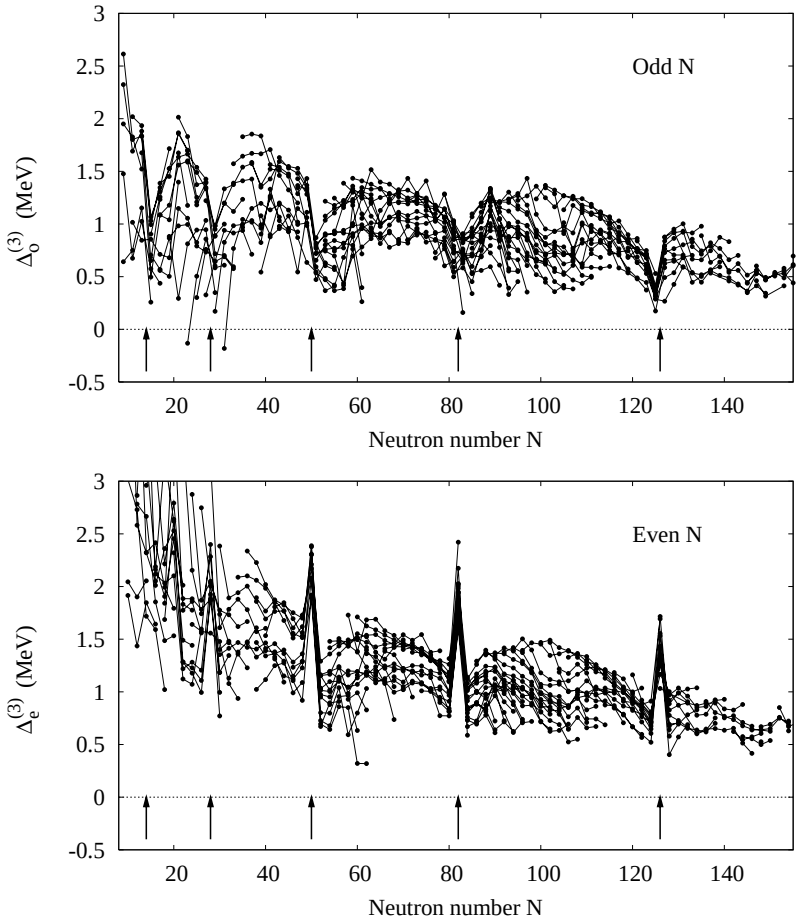

Fig. 1. Upper panels: odd-N pairing gaps. Lower panels: even-N pairing gaps.

factor of two scatter around the average value at a given N. Note that there are two exceptional cases with negative $\Delta^{(3)}$ for odd neutrons, at $N = 23$ and $N = 31$. I will come back them later. One can also see a systematic trend in the gap values as a function of N, namely the gaps get smaller in heavier nuclei. I will also come back to this behaviour in the theory discussion. Another feature of the odd-N gap systematics is the occurance of dips at particular values of N. In fact the dips occur adjacent to the well-known magic numbers $N = 28, 50, 82$ and 126. In addition there is a dip adjacent to $N = 14$, which corresponds to $n = 2$ in the magic number sequence $\frac{1}{3}(n + 1)(n^2 + 2n + 6)$.

The systematics of the even-N gaps shown in the lower panel is similar with respect to the following: average values, the fluctuations at each N, and the smooth trend downward with increasing N. However, the magic number anomolies are now very striking spikes that occur exactly at the magic numbers. Also, the average values in lighter nuclei appear to be larger for the even-N gaps than for the odd-N. I will also come back to this feature in the theory section.

The corresponding systematics of proton gaps is shown in Fig. 2. The same qualitative features are present here as well, but the magic number effects are less pronounced. I do not know of any explanation of this difference between neutron and proton pairing.

The table below gives some fits to the pairing gap systematics. Shown are the fitted values of the gap parameterizations and the rms errors of the fits, in units of MeV. The simplest model is a constant gap, $\Delta^{(3)} = C$, shown on the line labeled C. One sees that a typical gap size is 1 MeV, and typical fluctuations about that are smaller by a factor of 3. Beyond that, there are differences between protons and neutrons and between the odd and the even gaps. The even gaps are somewhat larger and have somewhat larger fluctuations, which is to be expected in view of the shell effects exhibited in Fig. 1. The odd proton gap is smaller than the odd neutron gaps which might be expected from the repulsive Coulomb contribution to the pairing interaction. There is also a mean-field contribution of the Coulomb that has opposite signs for even and odd protons. Indeed the even proton gaps are actually larger than their neutron counterparts.

For the next lines in the table, I come back to the broad trend in Fig. 1, a systematic decrease in gaps with increasing mass number. It is conventional to describe this with a fractional power dependence, $\Delta^{(3)} = c/A^{1/2}$. This decreases the rms errors somewhat, but there is no theoretical basis for the fractional power of A. In the last line I show the result of a two-parameter

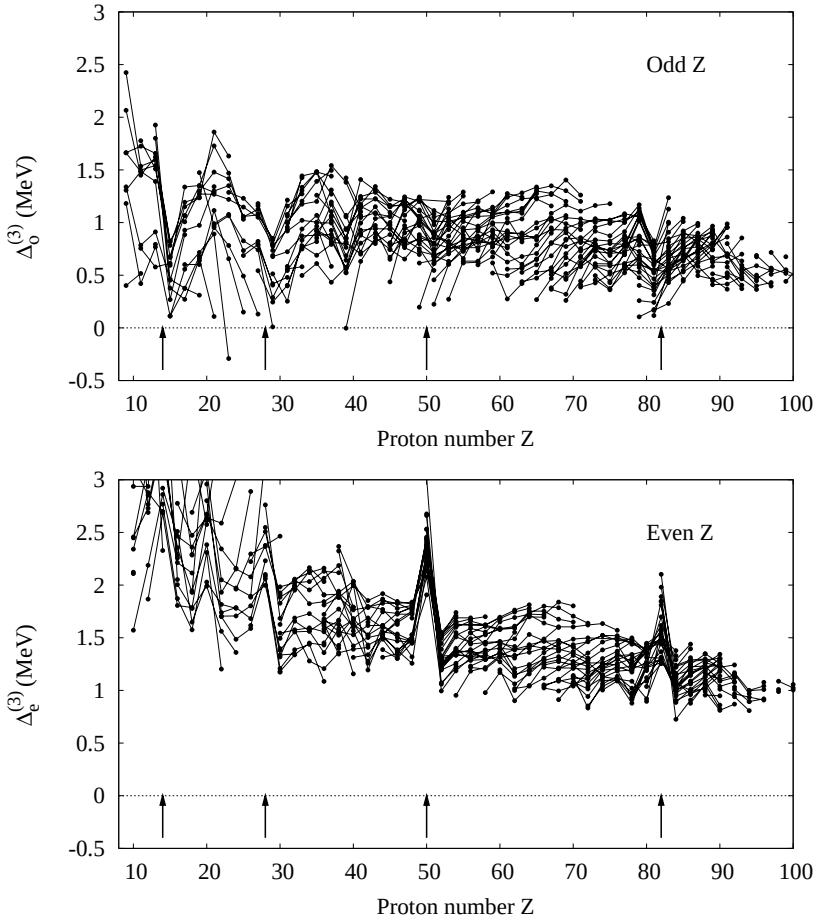

Fig. 2. Upper panels: odd-Z pairing gaps. Lower panels: even-Z pairing gaps.

fit to the functional form $\Delta^{(3)} = c_1/A + c_2$. This functional form is more justified by theoretical considerations, as will be discussed in the theory section below.

1.2. *Basic spectral properties*

The other strong signatures of pairing are in excitation spectra. In the simple BCS theory, the lowest excited states in an even system requires

$\Delta^{(3)}$	protons	protons	neutrons	neutrons
o/e	odd	even	odd	even
data set	418	407	443	442
C	0.96 ± 0.28	1.64 ± 0.46	1.04 ± 0.31	1.32 ± 0.42
$c/A^{1/2}$			$12/A^{1/2} \pm 0.25$	$12/A^{1/2} \pm 0.28$
$c_1/A + c_2$			$24/A + 0.82 \pm 0.27$	$41/A + 0.94 \pm 0.31$

breaking two pairs giving an excitation energy

$$E_{ex} \approx 2\Delta_{\rm BCS}. \tag{3}$$

On the other hand, in the odd particle number system, the quasiparticle level density diverges at the Fermi energy. This contrasting behavior is very obvious in the nuclear spectrum. As an example, the isotope chain at proton magic number $Z = 50$ (the element Sn) has been a favorite for exhibiting and studying pairing effects. Figure 3 shows the low-lying spectra of odd-N members of the chain. One can see that there are several levels within one MeV of the ground state. The spins and parities of the levels (not shown) correspond very well with the single-particle orbitals near the neutron Fermi level. However, the spectrum is very compressed with respect to orbital energies calculated with a shell model potential well. In contrast, the even members of the chain have no excited states at all within the excitation energy range displayed in the Figure.

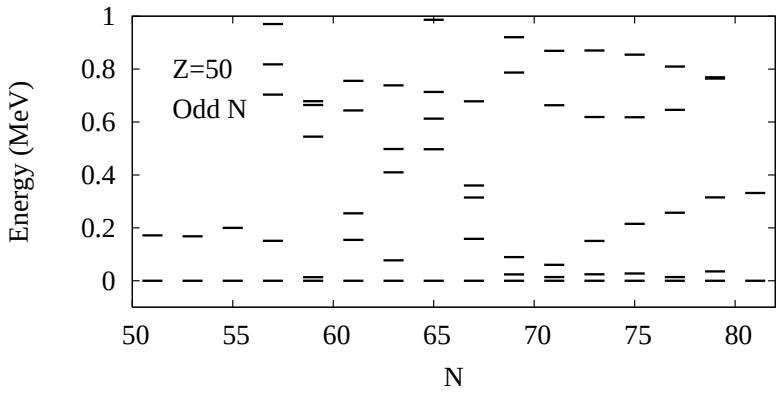

Fig. 3. Energy levels of odd-N Sn isotopes

Let us look now look at the global systematics for excitations in the

even-even nuclei. The estimate in Eq. (3) is too naive because there can be collective excitations within the gap, as is well-known from early days of BCS theory.[3] For example, there are longitudinal sound modes in an uncharged superfluid fermionic liquid. These have a phonon spectrum allowing frequencies within the quasiparticle gap. One might expect that such modes would be absent in finite systems when the size of the system is small compared to the coherence length of the pairing field. In fact the situation for nuclear excitations is much more complicated. However, just for presenting the systematics, we use the right-hand side of Eq. (3) to scale the excitation energies, taking the ratio $E_2/2\Delta$, where E_2 is the excitation energy and Δ is the smaller of $\Delta^{(3)}_{eZ}$ and $\Delta^{(3)}_{eN}$.

The scaled excitation energies of the first excited states in even-even are shown in Fig. 4. With only a few exceptions these states have angular momentum and parity quantum numbers $J^\pi = 2^+$ and can be considered to be collective quadrupolar excitations of the ground state. All of the

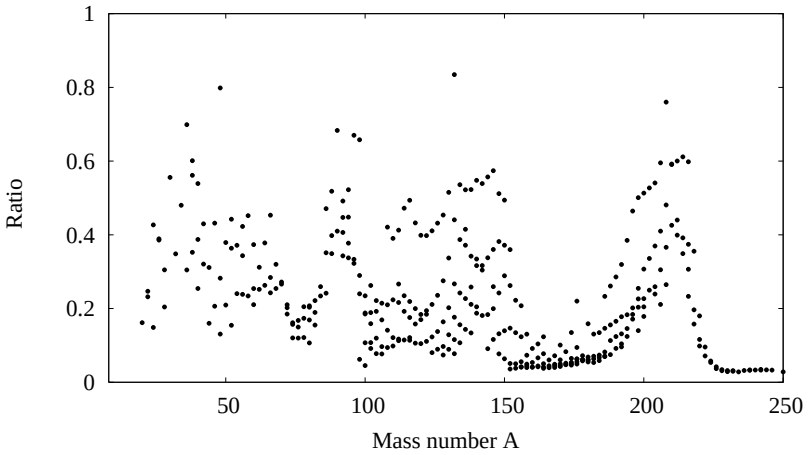

Fig. 4. Energy gap in the excitation spectrum of even-even nuclei, scaled to $2\Delta^{(3)}$. See text for details.

ratios are smaller than one, with most in the range 0.1-0.5. The very small excitations in the mass ranges $A = 160 - 180$ and $220 - 250$ correpond to nuclei with static quadrupole deformations.

The physics underlying these excitations is the softness of a typical nucleus with respect to quadrupolar deformations. On a qualitative level, the collectivity is similar to the phonon collectivity in the infinite Fermi gas. A

quantitative measure of the collectivity is the sum-rule fraction contained in the excitation, using the energy-weighted sum rule for some density operator. For the phonon case, the sum rule fraction approaches 100% when the frequency of the collective mode is small compared to the gap.[3] The collectivity in the nuclear quadrupole excitations is quite different. The sum rule fraction carried by the lowest 2^+ excitation is more or less constant over the entire range of nuclear masses, but it only about 10% of the total (for isoscalar quadrupole transitions. This is known as the Grodzins systematics.[4,5] The observed distribution of sum rule fractions is plotted as a histogram in Fig. 5.

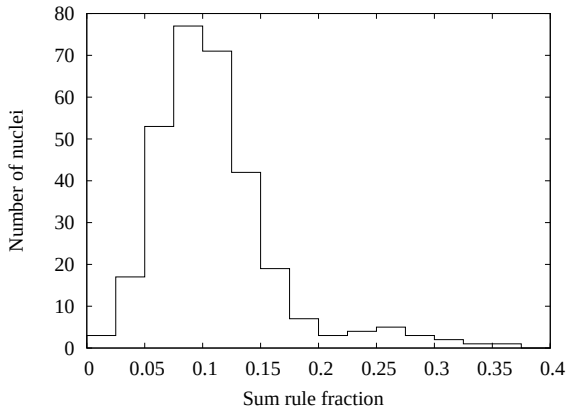

Fig. 5. Sum rule fraction for the first excited 2^+ state in even-even nuclei. See text for details.

Turning to odd-A spectrao, some systematics related to the level density are shown in Fig. 6. The average excitation energy of the first excited state is plotted for each odd mass number A, averaging over even values of Z. For comparison, the solid line is the expected spacing in the Fermi gas formula for the single-particle level density,

$$\frac{dn_s}{dE} = V\frac{mk_F}{2\pi^2} \approx \frac{A}{100} \text{ MeV}. \tag{4}$$

The subscript s on N_s indicates that only one spin projection is counted, and k_F is the Fermi momentum. V is the volume of the nucleus, which is (roughly) proportional to the number of nucleons A. One can see from the Figure that a typical spacing is a factor of 10 smaller than that given by the Fermi gas formula. Clearly interaction effects are at work to increase

the level density near the ground state.

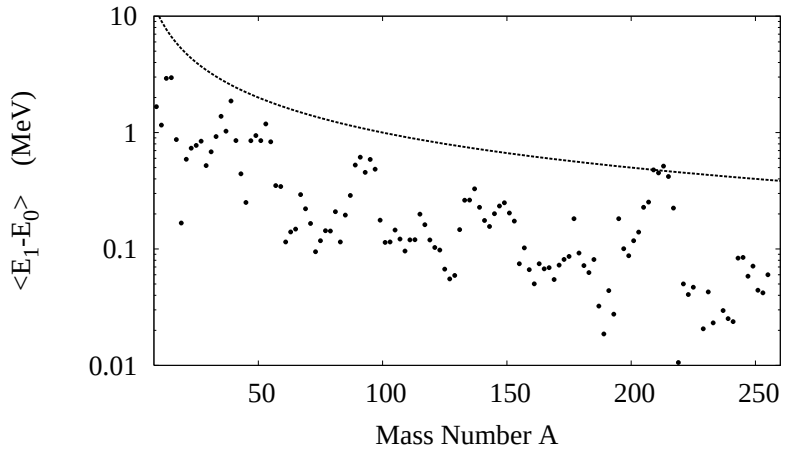

Fig. 6. Average energy of the first excited state in odd-A nuclei. The dashed line is the Fermi gas estimate, Eq. 4

2. Theory

Mean-field theory has made enormous strides in nuclear physics; the self-consistent mean field theory based on the Hartree-Fock-Bogoliubov approximation and using semi-phenomenological energy functionals is now the tool of choice for the global description of nuclear structure. It is not my intention to review this subject since it is well covered elsewhere in this volume.

Neverless, there are number of aspects of nuclear pairing that can be can rather easily understood using only the more qualitative aspects of pairing theory. Besides the pairing gaps and the effect on level densities, there are important consequences for two-nucleon transfer reactions and on dynamic properties such as radioactive decay modes. This section presents an overview of some of these aspects.

2.1. *Mean-field considerations*

BCS pairing is not the only source of odd-even staggering in binding energies. As is well-known in the physics of finite electronic systems, the Kramers degeneracy of single-particle orbitals gives rise to an odd-even effect. In a fixed potential well, the pair-wise filling of the orbitals makes

to a contribution to $\Delta_e^{(3)}$ that varies with system size as the single particle level spacing, $\Delta_e^{(3)} \sim A^{-1}$. In addition, the diagonal matrix elements of the two-body interaction in the Hartree-Fock orbitals also contribute to the odd-even staggering, both in $\Delta_o^{(3)}$ and in $\Delta_e^{(3)}$.[6] In the nuclear context, the volume occupied by the orbitals is (approximately) proportional to the mass number A, so this interaction contribution also varies as A^{-1}.

The last line of the Table shows a fit to the neutron pairing gaps including an A^{-1} term in the parameterization. It does almost as well as the phenomenological $A^{1/2}$ form. Note also that the coefficient of A^{-1} is larger for the even gaps than the odd ones. This is just what is to be expected from the contribution of the two-fold degenerate orbital energies.

Another mean field effect can be interpreted by Eq. (5,6) below, exhibiting the dependence of the pairing gap on the single-particle level densities. In general, level densities at the Fermi level are higher in spherical nuclei than in deformed nuclei because of the spherical shell degeneracy. Thus, one expects larger pairing gaps in spherical nuclei than in deformed. Even more dramatic is the shell quenching seen in the odd-N gaps in Fig. 1. The Fermi level in the spherical nuclei showing quenched gaps turns out to be in the $p_{1/2}$ or $s_{1/2}$ shell, which have low degeneracy. Thus, the occurance of the shell quenching is only partly due to the adjacent magic number.

2.2. *Strength of the pairing interaction*

The BCS theory gives the following formula for the gap parameter,[7]

$$\Delta_{\rm BCS} = (E_{max} - E_{min}) \exp(-1/g) \tag{5}$$

where

$$g = -G\frac{dn_s}{dE}. \tag{6}$$

Here the prefactor of the exponential is the window of single-particle energies for orbitals participating in the pairing and G is the strength of the pairing interaction. Eq. (6) defines the dimensionless quantity g that characterizes the strength of the pairing condensate.

In present-day theory, the qualitative formula Eq. (5) is superceded by detailed calculations of the orbitals and the pairing interaction, based on Hartree-Fock (HF) mean-field theory or Hartree-Fock-Bogoliubov (HFB) theory. This permits the treatment of the interaction by a two-nucleon potential and replacing of a generic level density by computed single-particle level spectra. However, there are significant uncertainties about both these

aspects, and the pairing interaction is often parameterized in a simple way. As an example, I show results of a global study of pairing systematics that used the Skyrme energy functional for the mean field and a contact interaction for the pairing.[8] The odd-N pairing gaps were calculated for two strengths of the pairing interaction, giving average gaps shown as the filled circles in Fig. 7. In the HFB calculations, the energy window was taken to be $E_{max} - E_{min} = 100$ MeV. Using this value in Eq. 5, the calculated average gap at $V_0/V_0^{sd} = 1$ is reproduced for $g = 0.20$. Noting that g depending linearly on the pairing strength, Eq. 5 gives the dashed line as a function of V_0. One sees that there is a very strong dependence of the gap on the pairing strength which is reproduced by the simple theory of Eq. 5. It is interesting to note also that Ref. [9][9] also estimated g as $g \approx 0.2$ using the meager data available at the time.

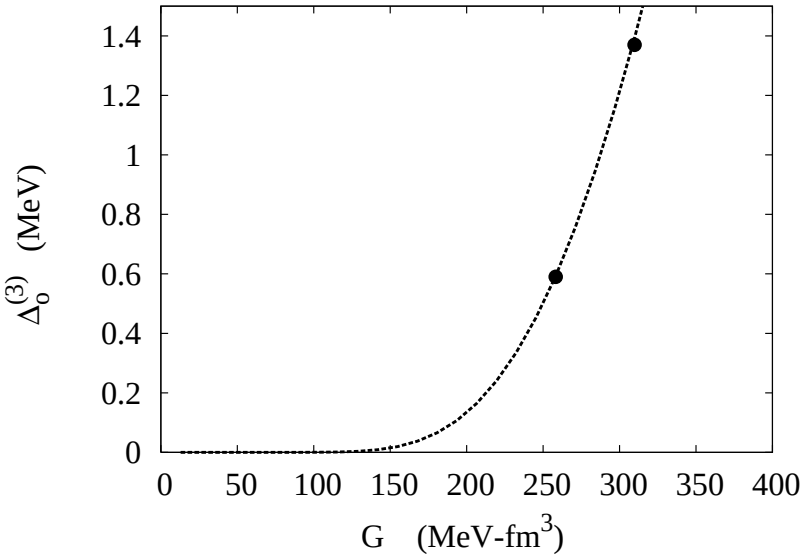

Fig. 7. Filled circles: average pairing gaps for 443 odd-N neutron gaps, calculated for two strengths of a contact pairing interaction.[8] Dot-dashed curve shows the dependence on strength according to eq. 5.

2.2.1. *Origin of the pairing interaction*

It is no surprise that conditions for pairing are satisfied in nuclei. The nuclear interaction between identical nucleons is strongly attractive in the spin-zero channel, almost to the degree to form a two-neutron bound state. While this explains the origin at a qualitative level, the many-body aspects of the nuclear interaction make it difficult to derive a quantitative theory starting from basic interactions. The progress one has made so far is reviewed in other chapters of this book, so I won't go into detail here. But just for perspective, I mention some of the major issues.

I first recall problems with the mean-field interaction to use at the Hartree-Fock level. Most obviously, the effective interaction between nucleons in the nuclear medium is strongly modified by the Pauli principle. The Pauli principle suppresses correlations between nucleons and that in turn make the effective interaction less attractive. Beyond that, it seems unavoidable to introduce three-body interactions in a self-consistent mean-field theory. These interactions have two origins. The first is the three-nucleon interaction arising from sub-nucleon degrees of freedom. It has been convincingly demonstrated that such interactions are needed to reproduce binding energies of light nuclei and to calculated the bulk properties of nuclear matter. Besides this more fundamental three-body interaction, there may an induced interaction associated with the short-ranged correlations and their suppression in the many-body environment. In the popular parameterization of the effective interaction for use in mean-field theory, the three-body interaction energy has the same order of magitude as the two-body interaction energy. It would thus seem to be a great oversimplication to ignore the three-body effects in the pairing interaction.

The last issue is the role of the induced interaction associated with low-frequency excitations. We have seen that the nucleus is rather soft to surface deformations. the virtual excitation of these modes would contribute to the pairing in exactly the same way that phonon provide an attractive pairing interaction for the electrons in a superconductor. The size of the induced interaction is estimated in Ref. [10];[10] it may well have the same importance as the two-particle interaction. Note that if low-frequency phonons were dominant, the energy scale in Eq. (5) would be greatly reduced.

2.2.2. *Spin-triplet pairing*

The strong attraction between identical nucleons was the starting point for the discussion of the pairing interaction in the previous section. In fact,

the attraction is even stronger between neutrons and protons in the spin $S = 1$ channel. Here the interaction gives rise to the deuteron bound state. Nevertheless, all the pairing phenomena seen above are a result of $S = 0$ pairing between identical nucleons.

This connundrum is resolved in two ways. First of all, pairing is only favored when all the particles can participate. The spin triplet interaction is only strong in neutron-proton pairs, so it would be suppressed in nuclei with a large imbalance between neutron and proton numbers. The other factor working against spin-triplet pairing is the spin-orbit field of the nucleus. It breaks the spin coupling of the pair wave function, but it is more effective in the spin-triplet channel.[11] In any case, an increase in nuclear binding energies is seen along the $N = Z$ line, called the "Wigner energy".[12]

2.3. *Dynamics*

The dynamic properties of an extended fermionic system depend crucially on the presence of a pairing condensate, changing it from a highly viscous fluid to a superfluid. The effects in nuclei are not quite as dramatic as in extended systems because the pairing coherence length in nuclei exceeds the size of the nucleus. Nevertheless, the presence of a highly deformable surface in nuclei requires that pairing be treated in a dynamical way.

2.3.1. *Rotational inertia*

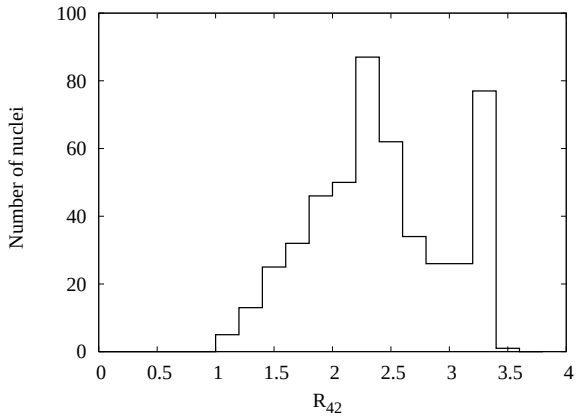

Fig. 8. Distribution of nuclei with respect to deformation indicator R_{42}

The most clearly documented dynamic influence of pairing is its effect on the moment of inertia of deformed nuclei. Without pairing, the rotational spectrum of a deformed fermionic droplet is believed to follow the spectrum of a rigid rotor,

$$E_J = \frac{\hbar^2}{2\mathcal{I}} J(J+1). \tag{7}$$

Here $\hbar J$ is the angular momentum and the moment of inertia $\mathcal{I}$ would be close to the rigid value

$$\mathcal{I} \approx \frac{2}{3} Am\langle r^2 \rangle \approx \frac{2}{5} A^{5/3} m r_0^2. \tag{8}$$

The author knows of no proof of this assertion, but it can derived from the cranking approximation applied to a many-particle wave function in a (self-consistent) deformed harmonic oscillator potential [13, pp. 77-78]. If the pairing were strong enough to make the coherence length small compared to the size of the system, the system would be a superfluid having irrotational flow and a corresponding inertial dynamics. What is somewhat surprising is that the weak pairing that is characteristic of nuclei still has a strong effect on the inertia.

One can separate out the deformed nuclei from the others by making use of the ratio excitation energies

$$R_{42} = \frac{E_4}{E_2}. \tag{9}$$

It is a good indicator of the character of the nucleus and has the value $R_{42} = 10/3$ for an axial rotor. A histogram of R_{42} for all the nuclei for which the energies are known is shown in Fig. 8. There is a sharp peak around the rotor value. The E_2 excitation energies of the nuclei corresponding to the peak are plotted in Fig. 9 as a function of A. Also plotted (dashed line) is the predicted value assuming a rigid rotor, Eq. (8). The experimental energies are systematically higher by a factor ~ 2, thus requiring inertias about half the rigid values. Present-day self-consistent mean-field theory is very successful in reproducing the experimental inertias, calculating them is what is called the self-consistent cranking approximation. As an example, the lower panel of Fig. 9 shows the calculated 2^+ energies using the HFB theory with an interaction that includes pairing.[14] The average energies are very well reproduced, and the rms errors in the energies are only $\pm 10\%$. While the theory works very well, it does not provide a parametric understanding of the dependence of the inertia on the pairing strength. Naively one might have expected that the effects would controlled

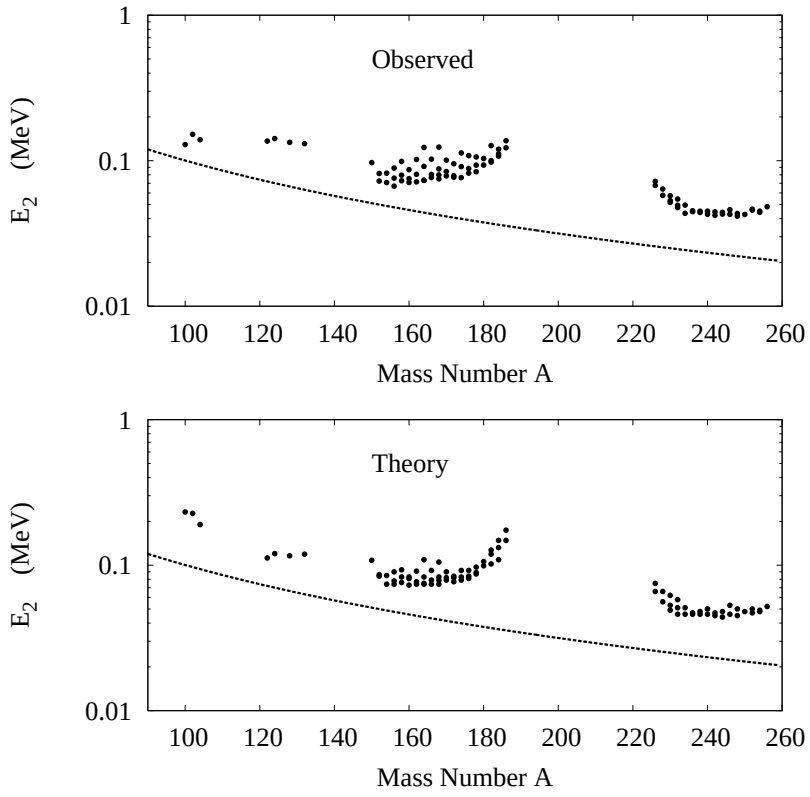

Fig. 9. Excitation energy of the first 2^+ state in deformed nuclei. The line shows the prediction assuming a rigid rotor.

by the ratio of the size of the nuclei to the coherence length of the Cooper pairs, which is a small number. We will also see in the next section another dynamic property showing a large influence of pairing.

2.3.2. *Large amplitude collective motion*

Also of interest, particularly in the theory of fission, is the effect of pairing on large-amplitude shape changes. Qualitatively, it is clear that pairing promotes fluidity. The degree to which this happens can be examined in one of the important observables of nuclear fission induced by low-energy excitation, such as occurs in neutron capture. The observable is the internal energy of the fission fragments. With nonviscous fluid dynamics,

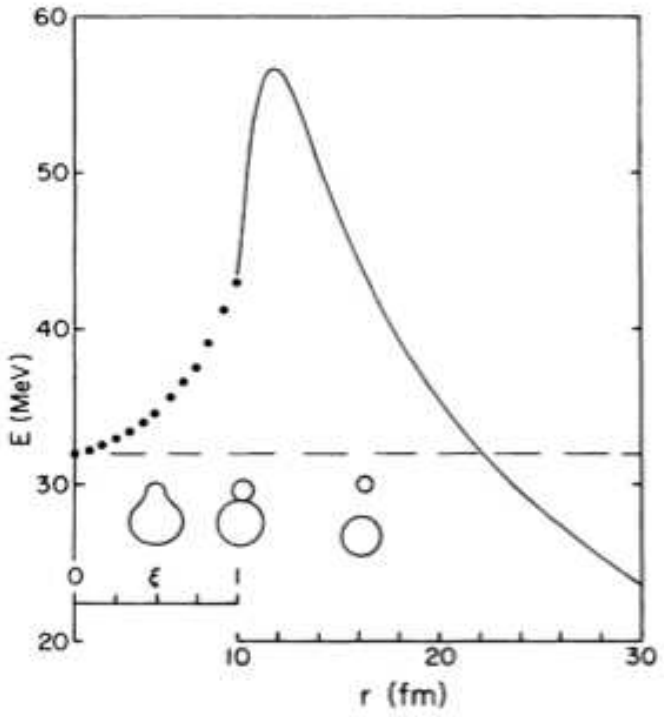

Fig. 10. Potential energy curve for the decay ^{223}Rn $\rightarrow$ ^{209}Pb + ^{14}C. The outside potential is a combination of Coulomb and nuclear heavy-ion potentials. The dots show the assumed Hartree-Fock states that connect the ground state 223Rn configuration to the final-state cluster configuration.

the internal energy would be largely deformation energy. With more viscous dynamics, there would be additional thermal energy. So far, one has not been able to perform realistic enough calculations to compare theory and experiment. But the computational tools for the time-dependent HFB theory are now reaching the point where such a test can be made. (See Chapter X in this book).

Spontaneous fission is a decay mode that requires the nucleus to tunnel under a barrier as it is changing shape. This kind of under-the-barrier dynamics is extremely sensitive to the character of the system, whether it is normal or superfluid. If the system is normal, the relevant configurations under the barrier are close to Hartree-Fock with relatively small interaction matrix elements mixing different configurations. On the other hand, if

there is pairing condensate, the interaction between configurations can be enhanced by a factor $2\Delta^2/G^2$ [10, p. 159, Eq. (7.8)], where here G is a typical interaction matrix element between neighboring mean-field configurations. Numerically, the pairing enhancement factor can be an order of magnitude or more. One should also keep in mind that in tunneling, the lifetime depends exponentially on the inertial parameters of the dynamics. As an example, the nucleus ^{234}U is observed to decay by many different channels, ranging from alpha decay to spontaneous fission, and including exotic modes such as emission of a Neon isotope. The observed lifetimes of these decays range over 12 order of magnitude. Theory including the enhancement factor is able to reproduce the lifetimes to within one or two orders of magnitude [10, p. 163, Table 7.1]. Without the enhancement factor, there would be no possibility to explain them.

Acknowledgment

I wish to thank A. Sogzogni for access to the NNDA data resources. I also thank A. Steiner and S. Reddy for helpful comments on the manuscript. This work was supported by the US Department of Energy under grant DE-FG02-00ER41132.

References

1. G. Audi, A. H. Wapstra, and C. Thibault, Nucl. Phys. A729, 337 (2003).
2. Brookhaven data base, http://www.nndc.bnl.gov/.
3. P.W. Anderson, Phys. Rev. **112** 1900 (1958).
4. L. Grodzins, Phys. Lett. **2**, 88 (1962).
5. S. Raman, C. Nestor, and P. Tikkanen, At. D. Nucl. D. Tables **78** 1 (2001).
6. T. Duguet, P. Bonche, P.H. Heenen, J. Meyer, Phys. Rev. C **65** 014311 (2001).
7. "Theory of Superconductivity", J.R. Schrieffer, (Benjamin, New York, 1964) p. 41, Eq. (34).
8. G.F. Bertsch, C.A. Bertulani, W. Nazarewicz, N. Schunck, and M.V. Stoitsov, Phys. Rev. C 79 034306 (2009).
9. A. Bohr, B. Mottelson, and D. Pines, Phys. Rev. **110** 936 (1958).
10. "Nuclear superfluidity : pairing in finite systems", D.M. Brink and R.A. Broglia., (Cambridge University Press, 2005).
11. A. Poves and G. Martinez-Pinedo, Phys. Lett. B 430, 203 (1998).
12. D. Lunney, J.M. Pearson and C. Thibault, Rev. Mod. Phys. **75** 1021 (2003).
13. A. Bohr and B. Mottelson, Nuclear Structure, Vol. II, (Benjamin, 1974).
14. J.-P. Delaroche, et al., Phys. Rev. C **81** 014303 (2010).